Research Article

Ayhan Etyemez*, Umut Aydin

Investigation of the effects of machining parameters on surface integrity in micromachining

https://doi.org/10.1515/chem-2022-0141
received January 27, 2022; accepted February 23, 2022

Abstract: In this study, the effect of cutting conditions on surface integrity was investigated in micromilling of magnesium alloy (AZ91). Microtool diameter, cutting speed, feed rate, and depth of cut parameters are used. These variables were investigated at three different levels with the Taguchi L_9 experimental design method. The least-best objective function was used. As a result of the experiments, surface roughness values were obtained. It has been determined that surface roughness values and depth of cut are effective parameters. After evaluating the results obtained, variance and regression analyses were performed. Based on the analysis of variance, 58.73% feed rate was found for the 1.0 mm diameter tool, on the other hand, for the 0.8 mm diameter tool, the depth of cut was found to be an effective parameter with 53.6%.

Keywords: machining parameters, surface integrity, micromachining

1 Introduction

Magnesium is an alkaline earth metal in group IIA of the periodic table. Magnesium has an atomic number of 12, an atomic weight of 24.3 g/mol, and a melting point of 651°C. Magnesium has the distinction of being the sixth most abundant metal and the eighth element, with a density of just 1.74 g/cm^3. Due to its lightness, its usage areas are quite high [1]. Magnesium is a silver-colored and shiny metal. When in contact with air, an oxide layer is formed on its surface. It is a refractory and easily formable material. It is 36% lighter than aluminum and 78% lighter than steel [2].

The use of magnesium continues to increase due to its properties in many sectors such as automotive, aerospace, defense, and machinery [3]. In the aviation industry, magnesium alloys are successfully used in aircraft skeleton, engine, gearbox, wheels, landing gear, interior furniture, cargo accessory products, ventilation, and pressurization systems [4]. Machining methods are used in the manufacture of magnesium alloys.

Machining is used extensively in aerospace, defense, electronics, medical, and automotive sectors. Miniaturization is frequently observed in the products of these sectors as well. Accordingly, machining started to be used on a microscale. With miniaturization, lightness, economy, superior surface quality, and precision are the desired features.

Micromachining is the name given to the process that enables miniaturization. Micromilling is the production of complex shaped parts with 1 mm or smaller tools with limited tolerances and high surface integrity. Ozel et al. modeled and simulated the micromilling process on Al 2024-T6 aluminum alloy and AISI 4340 steel. The diameter of the tool used in the research is 0.635 mm. Spindle speed is max 80,000 rpm. The impacts of spindle speed and feed ratio on the forces were investigated. A large fluctuation in cutting forces was observed due to process dynamics and continuous slip. The edge radius ratio of the minimum chip thickness was found to be between 42 and 45% for Al 2024-T6 aluminum alloy, and 30–35% for AISI 4340 steel [5]. The mechanistic force model presented by Mamedov and Lazoglu for micromilling gave more accurate results than the conventional force model. In the research, experiments were carried out on Al 7050 material. As a conclusion of the research, it was stated that the correct determination of the cutting forces is significant in terms of tool wear, product precision, and surface quality [6]. In a study conducted by

* **Corresponding author: Ayhan Etyemez,** Nikken Turkey, Istanbul, Turkey, e-mail: ayhan@nikken.com.tr
Umut Aydin: Marmara University, Faculty of Technology, Istanbul, Turkey

Open Access. © 2022 Ayhan Etyemez *et al.*, published by De Gruyter. This work is licensed under the Creative Commons Attribution 4.0 International License.

Mamedov and Lazoglu), they examined the techniques of measuring cutting force, tool elastic deformation, and speed of rotating tool. They stated the noisy force signal and the small band gap of the dynamometer as problems encountered when measuring cutting forces. They stated that in order to calculate the rotational speed of the tool, the laser beam is sent to the double-edged tool and the rotational speed of the tool can be calculated from the period of the displacement signal [7]. Oliaeia and Karpat conducted a micromilling study on Stavax stainless steel. In the experiments, the parameters of cutting speed, depth of cut, feed ratio, radial immersion percentage, and plunging method were investigated. Tool wear, machining forces, and surface roughness were analyzed. As a result of the experiments, the immersion method significantly affects the tool wear. Accordingly, surface quality and cutting forces are also affected. It has been demonstrated that the relationship between radial plunge and feed ratio is significant in terms of tool wear and surface roughness [8]. Gunaydin developed tool path geometry, machining strategy, and optimized cutting parameters in order to obtain maximum efficiency in the micro-groove milling process [9]. In the research, the values of cutting forces, surface roughness, and tool wear were not created by analytical calculation, but by mathematical models using an experimental design table. 2738 plastic die steel is used. With the aim of minimizing the manufacturing cost, the cutting parameters were optimized around this purpose. Cutter feed, cutting speed, and cutter diameter/groove width ratio are the parameters used. Models based on tool path geometry, which contain the response of the control unit to cutting conditions, have been developed [9]. Pratap et al. modeled cutting forces on Ti-6Al-4V alloy using ABAQUS program with finite element analysis. In the research, stress distribution, temperature distribution, and forces were simulated by using tool edge radius, uncut chip thickness, cutting speed, and feed ratio parameters. Maximum Von-Mises stress and cutting temperature are higher than that in macromilling of Ti-6Al-4V alloy. The reason for this is the tool edge radius and low feed values. The simulated cutting forces have been proven as a result of experiments [10]. Karpat et al. developed a mechanistic model based on the mean force model in which the tool axis deviation is included. In the study, it was stated that the cutting forces were not linear compared to milling at the macroscale. As a result of the studies on the Ti-6Al-4V alloy, it was observed that the force values obtained from the model revealed were compatible with the measured values [11].

Yucel and Cicek examined micromachining techniques commonly used in manufacturing. They have broadly classified micromachining techniques into two categories: micromachining and micro-abrasive machining. In the research, AISI H13 hardened (45 HRC) hot work tool steel was investigated by micromilling. It has been indicated that a better surface roughness can be obtained by optimizing parameters such as speed, axial depth, and the use of appropriate tool coatings in the micromilling process [12]. Aslantas et al. searched the effect of tool wear on groove geometry, surface quality, and burr formation in micromilling of Inconel 718 alloy. The experiments were carried out with constant cutting parameters and dry cutting conditions. In the research, the dimensional change, burr formation, and cutting forces in the groove obtained by micromachining were investigated. As a result of the experiments, it was observed that the cutting tool was worn axially and circumferentially [13]. Lu et al. investigated the effect of cutting parameters on microhardness and estimation of Vickers hardness based on reaction surfaces methodology in micromilling of Inconel 718 material. In the research, spindle speed, feed ratio, and axial depth parameters were used. As a result of the research, spindle speed affected Vickers hardness the most. Axial depth, on the other hand, affected more than the amount of feed. Microhardness decreases with increase in the spindle speed, and it increases with increase in the axial depth [14]. Aslantas and Kaynak examined the shape memory NiTi alloy with micromilling. Feed per tooth and depth of cut parameters were used in the research. Critical chip thickness was tried to be found. Burr width, cutting forces, and surface roughness are the outputs of the research. The critical chip thickness was obtained as 0.5 µm, as a result of the research. The critical chip thickness is 33% of the cutting-edge radius. As the cutting speed increases, the cutting force and burr widths also increase [15]. Kuram and Kesici researched the effects of cutting tool clamping length on tool wear, forces, and burr size in micromilling of Inconel 718 super alloy. Diameter reduction in the cutter was evaluated in determining tool wear. As a result of the research, it was determined that the measured Fx and Fy forces and burr width values of tool wear were proportional to the clamping length and increased with the increment in the clamping length. The lowest burr width was measured when the cutting tool clamping length was 10 mm [16]. Nahata et al. created a mathematical model of radial oscillation in the micromachining process, and then examined the radial oscillation with independent experiments and compared it with the mathematical

model [17]. Yu et al. investigated the impact of microstructure on surface integrity and chip form in the micromachining process. Copper material with two different grain sizes and a single diamond cutting tool were used in the research. Based on the research results, decreasing the grain size will reduce the effect of the microstructure on the surface integrity in the microcutting process. Moreover, it has been observed that the resulting chip shape loses continuity and becomes intermittent with the decrease in the feed rate for annealed and blister copper, which is the subject of the research. This observation was made for the same depth of cut [18]. Aslantas et al. examined the surface quality and burr width in micromilling in their study on Ti-6Al-4V alloy. Cutting parameters were optimized with the Taguchi method in the aim of minimum burr width and surface roughness. In the research, spindle speed, feed ratio, and depth of cut were used as parameters. As a result of the research, the feed was measured as 0.25 μm/step for the best surface quality. It was observed that ploughing occurred at a lower feed rate. Low feed and high depth of cut increase burr width. Furthermore, the increase in spindle speed causes rapid tool wear, resulting in an increase in burr width [19]. Sun et al. modeled micromilling on aluminum Al 7075-T6 material with finite element analysis. Cutting forces and chip formation were investigated with the change in feed rate in the research. It has been observed that as the radial depth of cut increases, the cutting forces increase [20]. Kuram and Ozcelik performed the optimization of spindle speed, feed rate, and depth of cut parameters using Taguchi experimental design method on Ti-6Al-4V and Inconel 718 materials [21]. Tool wear, surface roughness, and cutting forces were measured and then optimization was performed according to the signal/noise ratio. As a conclusion of the research, the spindle speed was determined as 12,000 rpm and the depth of cut was 75 μm for optimum surface roughness in Ti-6Al-4V titanium alloy. For Inconel 718 Nickel alloy, the spindle speed is determined as 10,000 rpm and the depth of cut is 75 μm. The feed rate for both materials was determined as 50 mm/min. The most significant parameter affecting tool wear is the depth of cut for Ti-6Al-4V and the spindle speed for Inconel 718 [21]. There are also few other studies done on this topics for different purposes [22–26].

In this study, the impact of cutting conditions on the surface integrity was investigated in the micro milling of magnesium alloy (AZ91). Microtool diameter, cutting speed, feed rate, and depth of cut parameters are used. These variables were investigated at three different levels with the Taguchi L_9 experimental design method. The least-best objective function was used. As a result of the experiments, the cutting force and surface roughness values were obtained. After evaluating the obtained results, variance analysis was performed. Lastly, the conclusion is conveyed.

2 Materials and methods

2.1 Materials

The material used in the research is the AZ91 series, which is a magnesium alloy. The components of the material are shown in Table 1 where the dimensions of the magnesium alloy used are 150 mm × 150 mm × 10 mm.

2.2 Experimental setup

For micromilling, it is necessary for the microcutting tools to work at high speeds. In the experiments, the Nikken brand spindle speeder was adapted for the CNC machining center as a high-speed rotation provider on the JOHNFORD VMC-850/550 + APC CNC Fanuc 0T x–y–z axis milling machine. The inner taper of the spindle speeder is in the norm of SK10. Collet in SK10 norm was used in order to use micro tools. 0.8 and 1 mm microtools were used in the experiments (Figure 1).

Kistler 9119AA1 dynamometer, Kistler 5080A type load amplifier, and DynoWare software program were used for the measurement of cutting force in the micromilling process of magnesium alloy. Surface roughness was measured with a Keyence digital microscope.

Table 1: AZ91 magnesium alloy and its chemical composition (wt%) [27]

Alloy element	Al%	Zn%	Mn%	Si% (max)	Fe% (max)	Cu%	Ni% (max)	Be%	Others%	Mg%
AZ91	8.5–9.5	0.45	0.17	0.05	0.004	0.025	0.001	—	0.01	Remaining

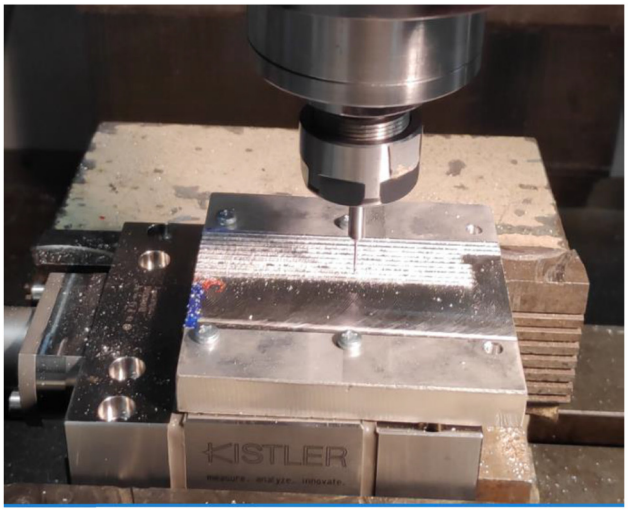

(a)



(b)




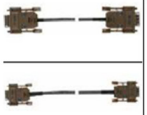

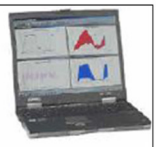

Dynamometer	Connection Cable	Amplifier	Connection Cable	DAQ System	Computer Dynoware Software
Type 9119AA1	Type 16xx	Type 5080A	Type 1700A111 A2	Type 5697A1	
			Type 1200A27		

(c)

Figure 1: Experimental setup: (a) experiment set, (b) cutting tool, and (c) cutting force measurement and evaluation set.

2.3 Experimental design

Parameters such as revs per minute, feed rate, and depth of cut constitute the cutting conditions. The Taguchi method reduces the number of experiments and provides a decrease in testing and production costs [28]. Experiments were designed using the Taguchi method. First, the control factor and levels were determined. Following this, matrix selection was made and the levels were transferred to the matrix. There are three different levels of variables according to the L_9 index used. A total of nine different experiments were conducted.

The variables and levels in this study are given in Table 2.

The list of experiments designed according to the Taguchi method is given in Table 3 below. The total number of experiments performed was nine.

Table 2: Variables and levels

Variables	Symbol	Units	Code	Levels		
				1	2	3
Rev	*n*	m/min	A	10,000	11,000	12,000
Feed rate	*f*	mm/min	B	170	200	230
Depth of cut	*d*	mm	C	0.1	0.2	0.3

Table 3: Experimental design

Experiment number	Variables	Cutting speed (m/min)	Feed rate (mm/rev.)	Depth of cut (mm)
1	A1B1C1	1	1	1
2	A1B2C2	1	2	2
3	A1B3C3	1	3	3
4	A2B1C2	2	1	2
5	A2B2C3	2	2	3
6	A2B3C1	2	3	1
7	A3B1C3	3	1	3
8	A3B2C1	3	2	1
9	A3B3C2	3	3	2

Table 4: Surface roughness and S/N values

Experiment number	Levels	1.0 mm tool		0.8 mm tool	
		R_a (μm)	S/N (dB)	R_a (μm)	S/N (dB)
1	A1B1C1	0.374	8.5426	0.407	7.8152
2	A1B2C2	0.370	8.6360	0.536	5.4167
3	A1B3C3	0.562	5.0053	0.256	11.8352
4	A2B1C2	0.227	12.8604	0.450	6.9357
5	A2B2C3	0.332	9.5772	0.455	6.8398
6	A2B3C1	0.440	7.1309	0.648	3.7752
7	A3B1C3	0.466	6.6323	0.332	9.5772
8	A3B2C1	0.310	10.1728	0.684	3.2989
9	A3B3C2	0.495	6.1079	0.310	10.1728

3 Results and discussion

3.1 Surface roughness results

The surface roughness values obtained as a result of the milling process on the magnesium AZ91 alloy according to the L_9 index and the S/N values calculated with the Taguchi least-best approach are given in Table 4.

In the measurements made with the Keyence device, five samples were taken for each experiment. The mean value of these samples was calculated and the results were conveyed. An image of the sample is given in Figure 2.

In Figure 3, the comparison of the surface roughness of the experiments with the 0.8 and 1.0 mm tools (time series plot of R_a) is given. It is observed that there is a similarity between the surface roughness values of the 4th, 5th, and 6th, 7th experiments. In Figure 4, a linear equation (fitted line plot) was obtained between the surface roughness values.

3.2 Surface roughness analysis

3.2.1 Main effects

When the experiments with the 1.0 mm tool were examined, the mean values of the obtained surface roughness values were between 0.22 and 0.56 μm. The S/N ratios of

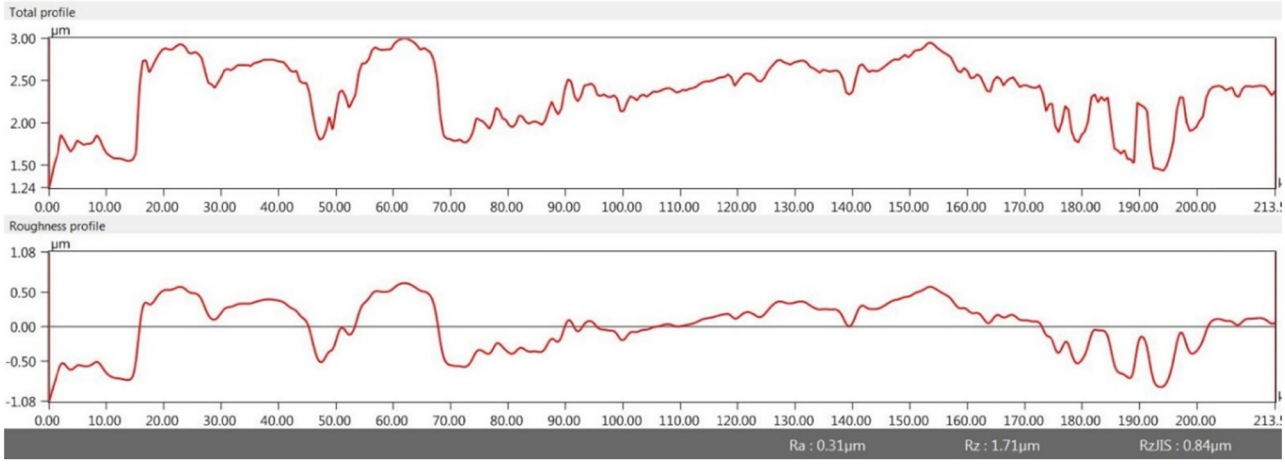

Figure 2: Surface roughness measurement.

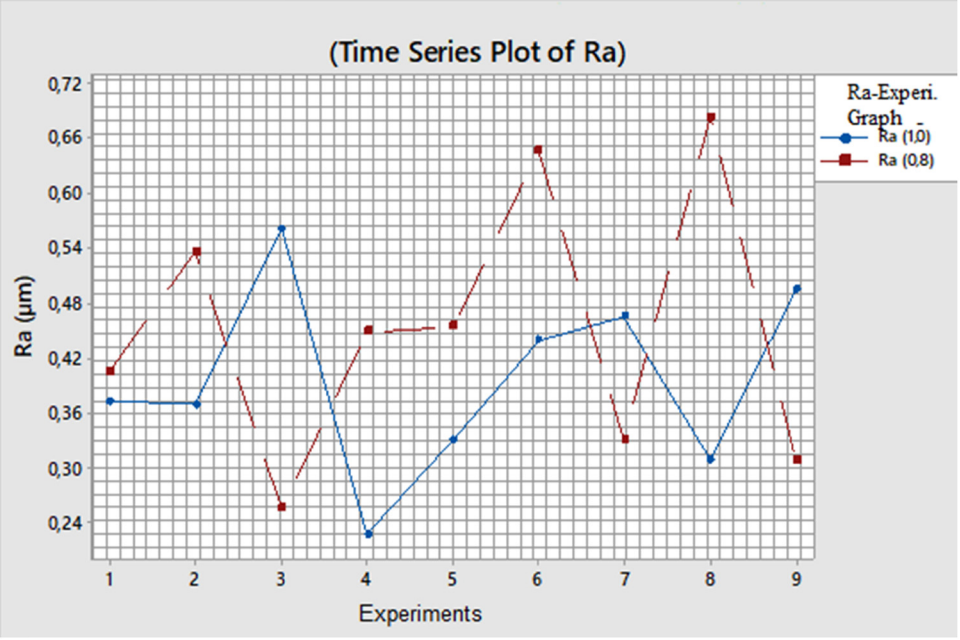

Figure 3: Comparison of surface roughness.

the surface roughness values according to the machining parameters are presented in Table 5 and Figure 5.

As seen in Table 5 and Figure 5, when the effects of machining parameters on the surface roughness are examined according to the obtained S/N ratio, it is seen that the lowest surface roughness value is obtained when the rev is 11,000 rpm, the feed rate is 170 mm/min, and the depth of cut is 0.3 mm (A2B1C3). Validation experiments were carried out for this. The obtained values are consistent with the literature [21,27,29].

When the experiments with the 0.8 mm tool were examined, the mean values of the obtained surface

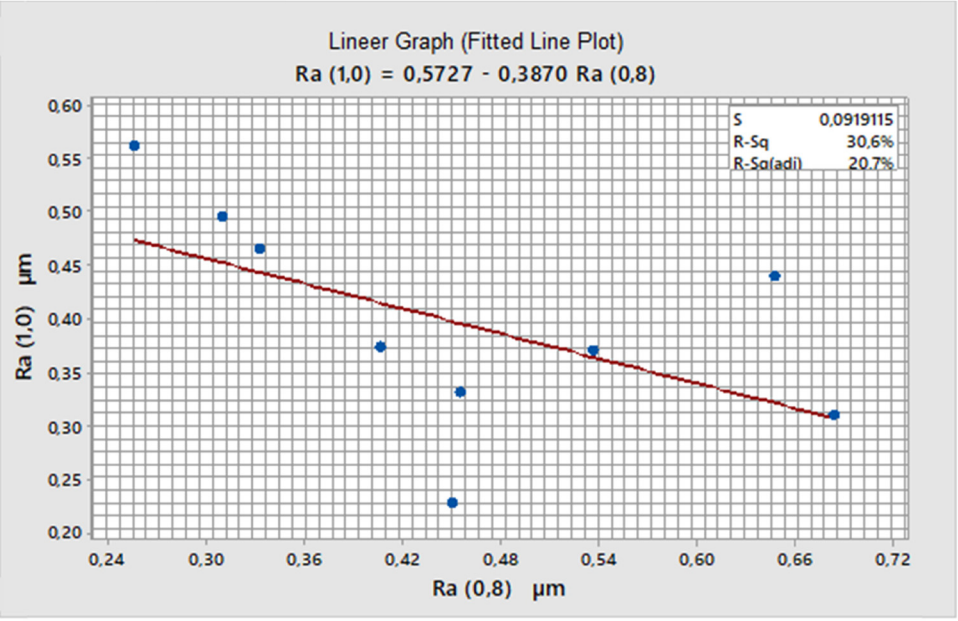

Figure 4: Comparison of surface roughness.

Table 5: S/N ratios of surface roughness values

Level	A rev (*n*) (rpm)	B feed rate (*f*) (mm/min)	C depth of cut (*d*) (mm)
1	7.395	9.345	8.615
2	9.856	9.456	9.201
3	7.638	6.081	7.072
Difference	2.462	3.381	2.13
Rank	2	1	3

Table 6: S/N ratios of surface roughness values

Level	A rev (*n*) (rpm)	B feed rate (*f*) (mm/min)	C depth of cut (*d*) (mm)
1	8.356	8.109	4.963
2	5.85	5.185	7.508
3	7.683	8.594	9.417
Difference	2.505	3.409	4.454
Rank	3	2	1

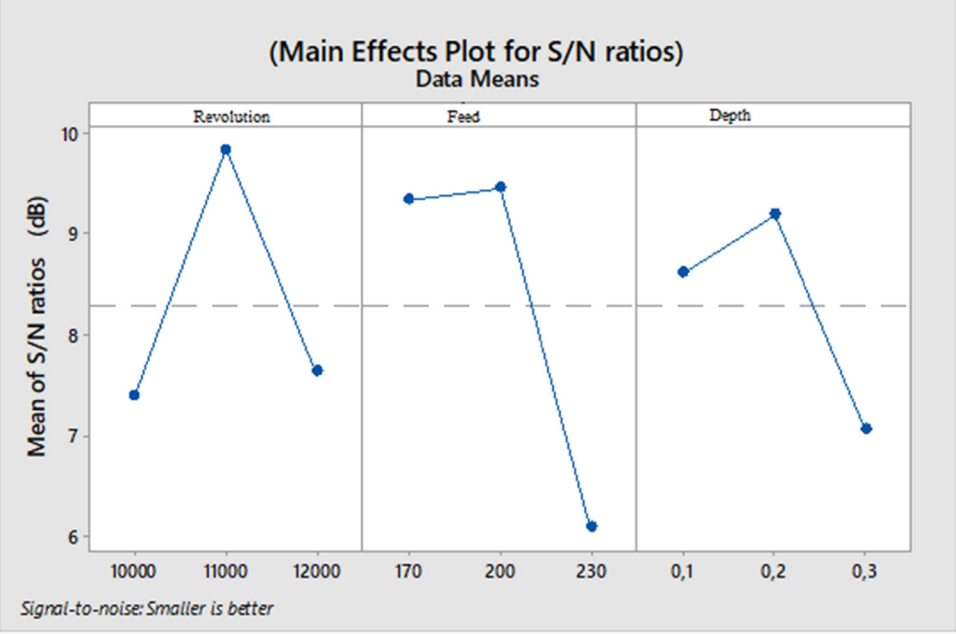

Figure 5: Main effect plot (1.0 mm).

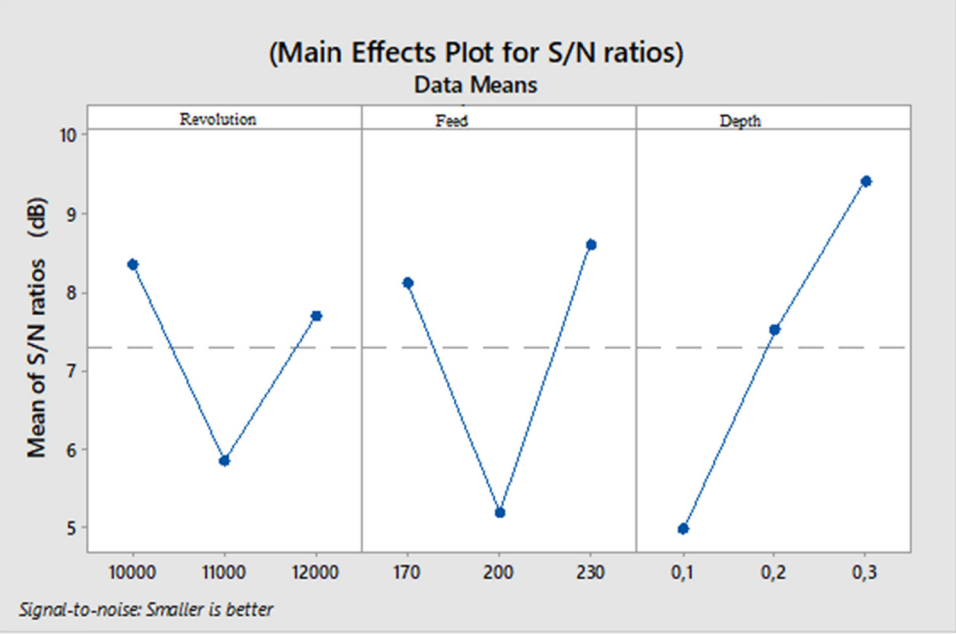

Figure 6: Main effect plot (for 0.8 mm tool).

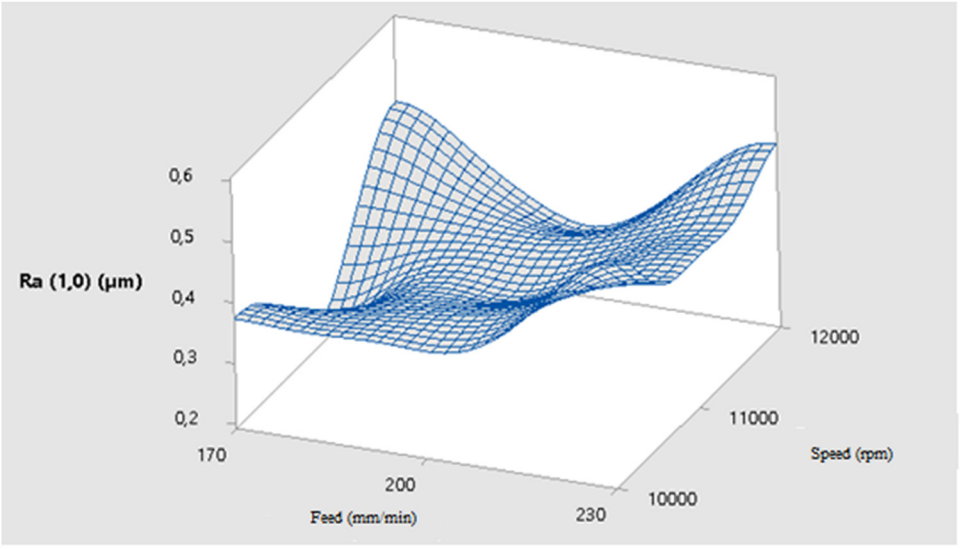

Figure 7: Effects of feed rate and rev on surface roughness.

roughness values were between 0.25 and 0.69 µm. S/N ratios of surface roughness values according to machining parameters are given in Table 6 and Figure 6.

The effects of machining parameters on the surface roughness are examined according to the S/N ratio obtained in the nine experiments performed with 0.8 mm tool, as seen in Table 6.

It is understood that the lowest surface roughness value is obtained when the rev is 12,000 rpm, the feed rate is 200 mm/min, and the depth of cut is 0.3 mm (A3B2C1). Validation experiments were carried out for this.

3.2.2 Effect plots

As seen in Table 5, in the experiments performed with the 1.0 mm tool, the feed parameter has the greatest effect on the cutting force. Thereafter, rev and depth of cut are significant. The effects of the parameters used in the experimental studies on the cutting forces are given in Figures 7–9.

As seen in Table 6, the effect of the cutting depth parameter on the cutting force is the highest in the experiments performed with the 0.8 mm tool. Following this, feed and rev are important. The effects of the

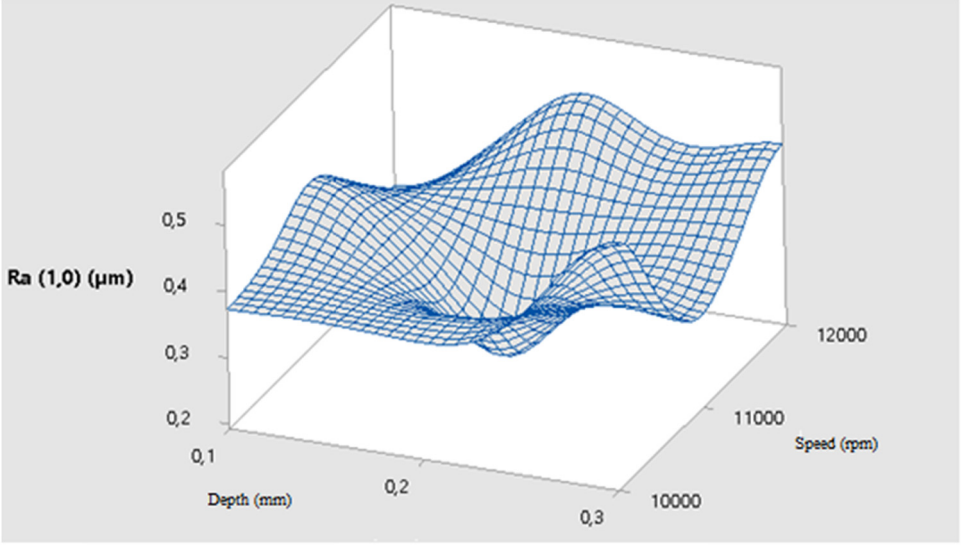

Figure 8: Effects of depth of cut and rev on surface roughness.

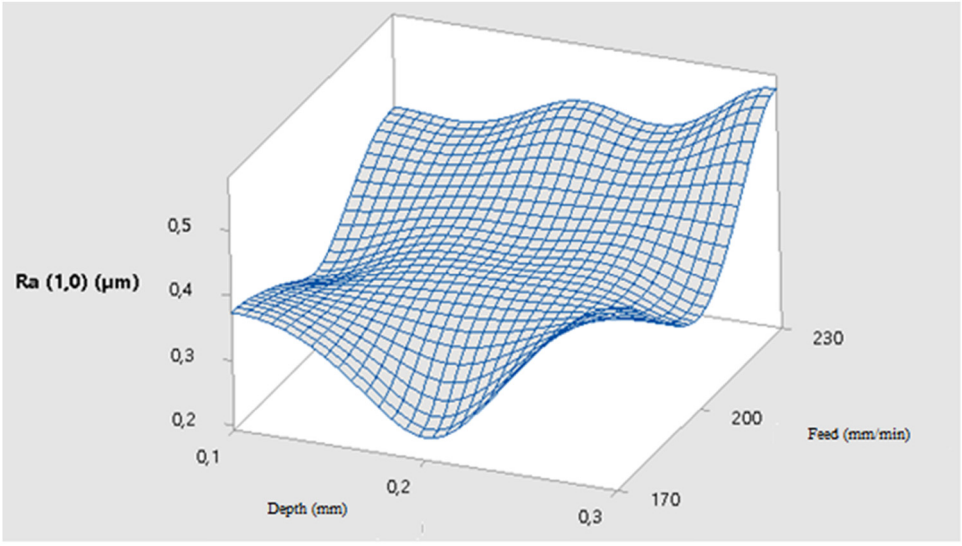

Figure 9: Effects of the depth of cut and feed rate on surface roughness.

parameters used in the experimental studies on the cutting forces are given in Figures 10–12.

3.2.3 Variance analysis

The results of the variance analysis of the mean surface roughness values in the experiments performed with the 1.0 mm tool are shown in Table 7. As can be interpreted from the table, the most effective factor in the formation of roughness on the machined surface as a result of machining AZ91 magnesium alloy material with micro-cutting tools is the feed with 58.73%.

The results of the mean surface roughness variance analysis of the experiments performed with a 0.8 mm tool are shown in Table 8. As can be seen from the table, unlike the experiment results processed with 0.8 mm, the most effective factor is the depth of cut with 53.60%.

As a result of the experiments, feed rate is a parameter that affects the surface roughness. It is observed that the depth of cut for the 0.8 mm tool affects the surface roughness.

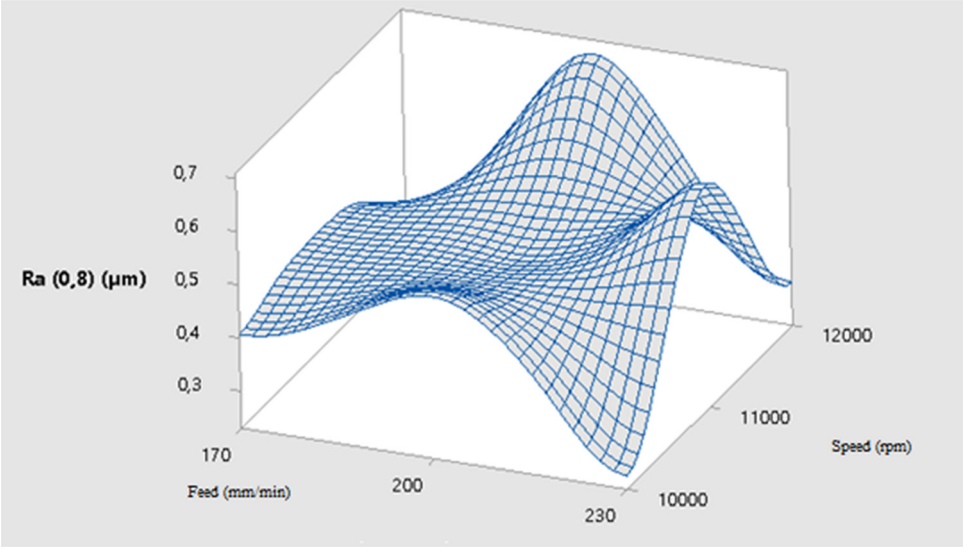

Figure 10: Effects of feed and rev on surface roughness.

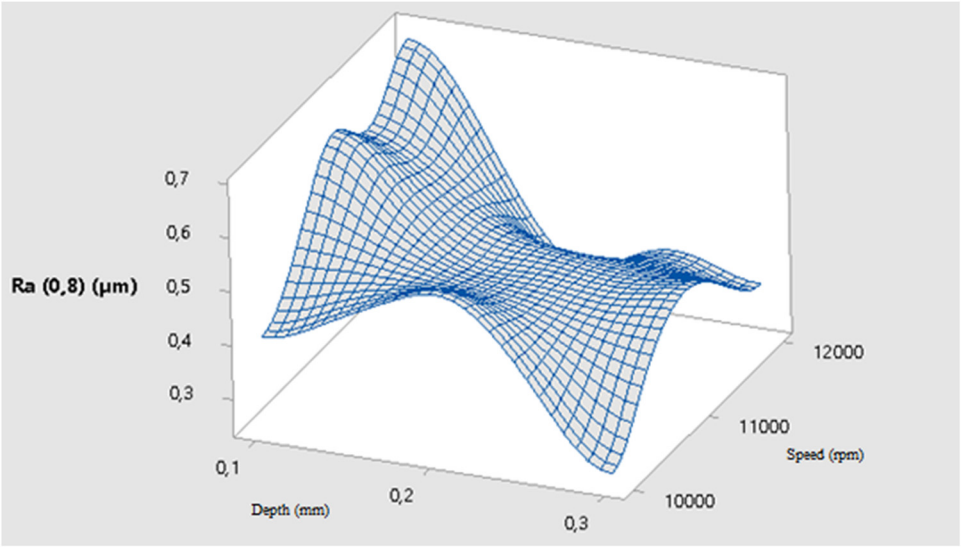

Figure 11: Effects of depth of cut and rev on surface roughness.

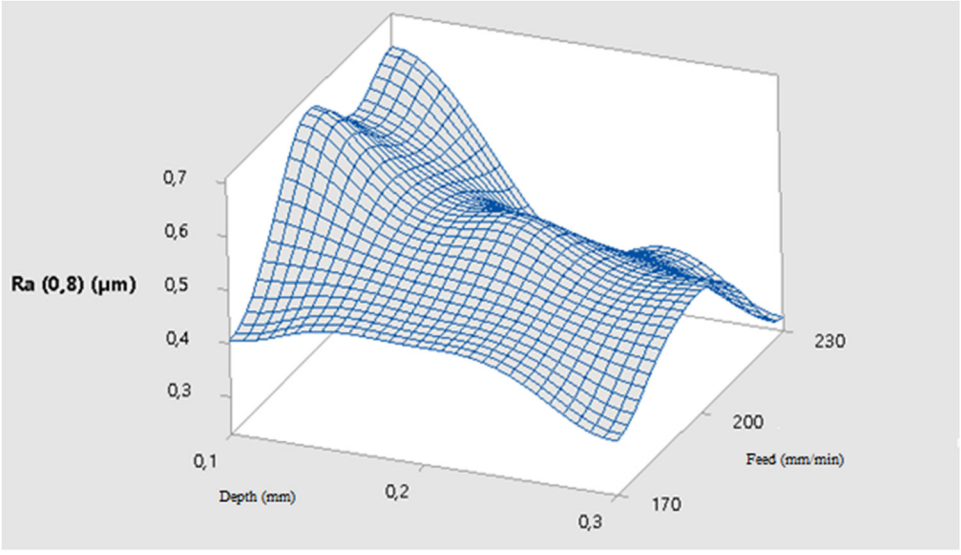

Figure 12: Effects of depth of cut and feed rate on surface roughness.

Table 7: Surface roughness ANOVA results 1 mm tool

Parameter	Degree of freedom	Sum of squares	Mean of squares	*F* value	%
Rev (*n*)	2	0.018764	0.009382	3.59	23.48
Feed (*f*)	2	0.046975	0.023488	8.98	58.73
Depth (*d*)	2	0.014249	0.007125	2.72	17.79
Error	2	0.005231	0.002616		
Total	8	0.08522			

Table 8: Surface roughness ANOVA results of 0.8 mm tool

Parameter	Degree of freedom	Sum of squares	Mean of squares	*F* value	%
Rev (*n*)	2	0.02141	0.01071	1.06	13.90
Feed (*f*)	2	0.05001	0.02501	2.48	32.50
Depth (*d*)	2	0.08253	0.04127	4.09	53.60
Error	2	0.02018	0.01009		
Total	8	0.17414			

Table 9: Optimum levels for surface roughness

Parameters	Symbol	Units	Code	For 1.0 mm tool		For 0.8 mm tool	
				Optimum level	Optimum value	Optimum level	Optimum value
Rev	n	rpm	A	2	11,000	1	12,000
Feed	f	mm/min	B	2	170	1	200
Depth	d	mm	C	2	0.3	3	0.1

Table 10: Validation experiments

A3B1C1 level	For 1.0 mm tool		For 0.8 mm tool	
	R_a (μm)	S/N (dB)	R_a (μm)	S/N (dB)
Calculated value	0.240	11.927	0.237	11.290
Validation experiments results	0.256	11.836	0.262	11.634
Differences	0.016	0.091	0.025	0.344

3.2.4 Optimization

Optimum levels of surface roughness are given in Table 9 for 1.0 mm tool and 0.8 mm tool. These levels were obtained from Tables 5 and 6. A2B1C3 is the optimum level for a 1.0 mm tool. For a 0.8 mm tool, on the other hand, A3B2C1 is the optimum level.

3.2.5 Validation experiments

The value validation experiments were carried out in which the roughness value was estimated by Minitab linear regression under optimum conditions. As a result of the regression estimation at the A2B1C3 level for the 1.0 mm tool, the surface roughness value of 0.240 μm was obtained, and for the 0.8 mm tool, surface roughness value of 0.237 μm at the A3B2C1 level was obtained. As a result of the validation experiments, the surface roughness values were found as 0.256 μm for the 1.0 mm tool and 0.262 μm for the 0.8 mm tool. The obtained values are consistent with the literature. [21,29]. The results are presented in Table 10.

Estimates for the 1.0 mm tool have an error of 6.70% according to the validation experiment. This value is 9.5% for a 0.8 mm tool.

3.2.6 Regression analysis

The equations obtained for the surface roughness values as a result of the linear regression analysis are given below. The equations stated in 1 and 2 were obtained with three unknowns with the rev feed and depth parameters. The equations specified in 3 and 4 represent a quadratic equation and also include the relationship of the parameters with each other.

For experiments with a 1.0 mm tool:

$$R_a = -0.094 - 0.000006 \cdot n + 0.00239 \cdot f + 0.393 \cdot d, \quad (1)$$

$$R_a = 21.19 - 0.003027 \cdot n - 0.04613 \cdot f + 1.815 \cdot d + 0.000100 \cdot f^2 + 6.675 \cdot d^2 + 0.000001 \cdot n \cdot f - 0.01961 \cdot f \cdot d. \quad (2)$$

For experiments with 0.8 mm tool:

$$R_a = 0.424 + 0.000021 \cdot n + 0.00014 \cdot f - 1.159 \cdot d, \quad (3)$$

$$R_a = -21.22 + 0.002153 \cdot n + 0.09982 \cdot f + 1.461 \cdot d - 0.000176 \cdot f^2 - 0.4861 \cdot d^2 - 0.000002 \cdot n \cdot f - 0.01394 \cdot f \cdot d. \quad (4)$$

The obtained values are consistent with the literature [28].

4 Conclusion

In this study, Taguchi (L_9) experimental design was made for three different levels of rev, feed, and depth of cut parameters. A total of 18 experiments were conducted at three different levels for two different tools. As the surface roughness value is desired to be minimum, the smallest best objective function is used [19,21]. The results for both tools were examined and analyzed separately.

When the mean surface roughness values of the experiments performed with the 1.0 mm tool were examined, the maximum surface roughness of 0.56 μm was obtained in the third experiment, and the minimum surface roughness of 0.22 μm was obtained in the fourth

experiment. The mean surface roughness in the experiments is 0.40 µm.

When the mean surface roughness values of the experiments performed with a 0.8 mm tool were examined, the maximum surface roughness of 0.68 µm was obtained in the eighth experiment and a minimum surface roughness of 0.25 µm was obtained in the third experiment. The mean surface roughness in the experiments is 0.45 µm.

When the mean values of the surface roughness are compared, higher roughness values were observed in the experiments performed with the 0.8 mm tool. One reason for this may be the vibration during machining caused by the increased rev parameter.

It is observed that there is a similarity between the surface roughness values of the 4th, 5th, and 6th, 7th experiments. The equation specified in (equation (5)) was obtained linearly between the surface roughness values.

$$R_a(1.0) = 0.5727 - 0.387 \cdot R_a(0.8), \quad (5)$$

When the research is evaluated in terms of surface roughness, the most effective factor for the 1.0 mm tool is feed rate with 58.73%. The effect of feed on the surface roughness is expected and is a situation in the literature [27,28]. Thereafter, rev and depth are significant. The most effective factor for the 0.8 mm tool is the depth of cut with 53.60%, followed by feed and rev. As can be understood, the depth parameter has a great effect on the tool surface roughness of 0.8 mm.

In experiments (A2B1C3) using 1.0 mm tool, it has been observed that minimum surface roughness can be obtained with 11,000 rpm, 170 mm/min feed, and 0.3 mm depth of cut. On the other hand, in experiments using 0.8 mm tool (A3B2C1), it was observed that minimum surface roughness could be obtained with 12,000 rpm, 200 mm/min feed, and 0.1 mm depth of cut. Unlike the literature, an increase in surface roughness values was observed at low depth of cuts due to scraping and friction.

It is demonstrated in the study that the Taguchi optimization technique is an effective technique in the machinability of AZ91 magnesium alloy material, in the experimental design, and in the optimization of the parameters and the response values in the desired ratios [19,21,29–31].

Acknowledgements: There is no body or organization to be acknowledged.

Funding information: There are no funding sources for this study.

Author contributions: All data were obtained by authors equally.

Conflict of interest: The authors declare that they have no known competing financial interests or personal relationships that could have appeared to influence the work reported in this article.

Ethical approval: The conducted research is not related to either human or animal use.

Data availability statement: All data generated or analyzed during this study are included in this published article.

References

[1] Kaçar İ, Öztürk F. Magnezyum alaşimlarinin şekillendirilmesindeki son gelişmeler. TİMAK-Tasarım İmalat Anal Kongresi. 2006. p. 354–61 (Turkish).

[2] Gözüaçık NK. AZ91 magnezyum alaşiminin mikro ark oksidasyonunda elektrolit bileşiminin etkileri. Yüksek lisans tezi. İstanbul: İstanbul Teknik Üniversitesi, Fen Bilimleri Enstitüsü, Metalürji ve Malzeme Mühendisliği Anabilim Dalı; 2012 (Turkish).

[3] Atalay O. Magnezyum ve alaşimlarinin konstrüksiyon malzemesi olarak otomotivde kullanimi. Yüksek lisans tezi. Istanbul: İstanbul Teknik Üniversitesi, Fen Bilimleri Enstitüsü, Makine Mühendisliği Anabilim Dalı, İstanbul Türkiye; 2006 (Turkish).

[4] Güler KA. Uçak Yapımında Kullanılan Malzemeler ve Özelliklerinin İncelenmesi. Bitirme Tezi, Yıldız Teknik Üniversitesi, Kimya-Metalürji Fakültesi, Metalürji ve Malzeme Mühendisliği Bölümü. İstanbul: Türkiye; 2003 (Turkish).

[5] Özel T, Liu X, Dhanorker A. Modelling and simulation of micro-milling process. Mater Manuf Process. 2009;24(12):1–8.

[6] Mamedov A, Lazoğlu İ. Mikro Frezeleme İçin Mekanistik Kuvvet Modeli. 3. Ulusal Tasarım İmalat ve Analiz Kongresi. Balıkesir: Türkiye; 2012;29–30 Kasım 2012, Turkish.

[7] Mamedov A, Lazoğlu İ. CNC ile Talaşlı İşlemede Kuvvet ve Titreşim Ölçümü. VIII. Ulusal Ölçümbilim Kongresi. Gebze/Kocaeli; 2013;26–28. Kocaeli: Eylül 2013, Turkish.

[8] Oliaeia SN, Karpat Y. Experimental investigations on micro milling of Stavax stainless steel. Procedia CIRP. 2014;14:14377–82. doi: 10.1016/j.procir.2014.03.006.

[9] Günaydın E. Mikro frezeleme uygulamalarinda. uygun takim yolunun ve kesme parametrelerinin belirlenmesi. Kocaeli, Türkiye: Yüksek Lisans Tezi, Gebze Yüksek Teknoloji Enstitüsü, Makine Mühendisliği Anabilim Dalı; 2014 (Turkish).

[10] Pratap T, Patraa K, Aleksandr D. Modeling cutting force in micro-milling of Ti-6Al-4V titanium alloy. Procedia Eng. 2015;129:134–9. doi: 10.1016/j.proeng.2015.12.021.

[11] Karpat Y, Kanlı M, Oliaer SN. Mikro frezeleme işleminin takım eksen sapması göz önüne alınarak mekanistik modellemesi. J Faculty Eng Architecture Gazi Univ. 2018;3(2):771–81 (Turkish).
[12] Yücel E, Çiçek A. İmalat alaninda yaygin olarak kullanilan mikro işleme teknikleri. Sakarya Üniversitesi Fen Bilimleri Derg. 2011;15(1):46–59 (Turkish).
[13] Aslantaş K, Çiçek A, Çelik SG. Mikro işlemede takim aşinmasi-kanal geometrisi ilişkisi üzerine deneysel bir çalişma. J Faculty Eng Architecture Gazi Univ. 2018;33(4):1285–98.
[14] Lu A, Jia Z, Wanga H, Feng Y, Liang SY. The effect of cutting parameters on micro-hardness and the prediction of Vickers hardness based on a response surface methodology for micro-milling Inconel 718. Measurement. 2019;140:56–62. doi: 10.1016/j.measurement.2019.03.037.
[15] Aslantaş K, Kaynak Y. Şekil hafızalı NiTi alaşımının mikro frezelenmesi ve kritik talaş kalınlığının belirlenmesi. J Faculty Eng Architecture Gazi Univ. 2019;34(3):1201–11 (Turkish).
[16] Kuram E. Kesici takim bağlama uzunluğunun mikro frezelemede takim aşinmasi. Kuvvetler ve Çapak Boyutu Üzerindeki Etkileri Dokuz Eylül Üniversitesi Mühendislik Fakültesi Fen ve Mühendislik Derg. 2017;19(55):229–37 (Turkish).
[17] Nahata S, Onler R, Korkmaz E, Ozdoganlar OB. Radial throw at the cutting edges of micro-tools when using ultra-high-speed micro machining spindles. Proc Manuf. 2018;26:1517–26. doi: 10.1016/j.promfg.2018.07.085.
[18] Yu J, Wang G, Rong Y. Experimental study on the surface integrity and chip formation in the micro cutting process. Proc Manuf. 2015;1:655–62. doi: 10.1016/j/promfg.2015.09.063.
[19] Aslantaş K, Ekici E, Çiçek A. Optimization of process parameters for micro milling of Ti-6Al-4V alloy using Taguchi-based gray relational analysis. Measurement. 2018;128:419–27. doi: 10.1016/j.measurement.2018.06.066Get.
[20] Sun Q, Cheng X, Liu Y, Yang X, Li Y. Modelling and simulation for micromilling mechanisms. Procedia Eng. 2017;174:760–6. doi: 10.1016/j.proeng.2017.01.219.
[21] Kuram E, Ozçelik B. Optimization of machining parameters during micro-milling of Ti6Al4V titanium alloy and Inconel 718 materials using Taguchi method. Proc Inst Mech Eng, Part B: J Eng Manuf. 2015;231(2):228–42. doi: 10.1177/0954405415572662.
[22] Singh SK, Panda SK, Singh SK, Panda SK. An analytical approach to evaluate the effective coefficients of piezoelectric composites. Emerg Mater Res. 2021;10(2):178–93. doi: 10.1680/jemmr.19.00167.
[23] Dindar B, Ağir İ, Dindar B, Ağir İ. Tensile and buckling properties of notched 6063 aluminum repaired with composite patches. Emerg Mater Res. 2021;10(2):139–44. doi: 10.1680/jemmr.20.00306.
[24] Kurtulmuş M, Doğan E;, Kurtulmuş M, Doğan E. The effects of undercut geometry on the static stress concentration factor of welds. Emerg Mater Res. 2021;10(3):272–7. doi: 10.1680/jemmr.20.00100.
[25] Yusuf D, Bekir G, Adem Ö, Ali Ö. Microstructure and wear properties of WC–10Co–4Cr coating to cultivator blades by DJ-HVOF. Emerg Mater Res. 2021;10(3):278–88. doi: 10.1680/jemmr.20.00324.
[26] Berkant D, İnan A, Behlül BN. Low-velocity impact response of Kevlar/epoxy aluminum laminates. Emerg Mater Res. 2021;10(3):295–9. doi: 10.1680/jemmr.20.00302.
[27] Aydın U, Ay M, Etyemez A. Milling of magnesium alloy with micro cutting tools. Int J Innovative Res Rev. 2019;3(1):30–4.
[28] Ay M, Ay İ. The prediction and optimization of the effects of abrasive waterjet cutting parameters on kerf. Acta Phys Pol A. 2016;129(4):762–6. doi: 10.12693/APhysPolA.129.762.
[29] Akgün M, Özger G, Ulaş HB. Döküm yöntemiyle üretilmiş AZ91 magnezyum alaşiminin işlenebilirliğinin yüzey pürüzlülüğü açisindan değerlendirilmesi. Erciyes Üniversitesi Fen Bilimleri Enstitüsü Derg. 2014;30(5):323–8 (Turkish).
[30] Basmacı G, Taskin A, Koklu U. Effect of tool path strategies and cooling conditions in pocket machining of AZ91 magnesium alloy. Indian J Chem Technol. 2019;26(2):139–45.
[31] Basmaci G. Optimization of processing parameters of AISI 316 Ti stainless steels. Academic Platf J Eng Sci. 2018;6(3–6):1–7. doi: 10.21541/apjes.422606.